

SYNTHESES AND CHARACTERIZATION OF BIRNESSITE BY OXIDIZING PYROCHROITE IN ALKALINE CONDITIONS

DENG S. YANG AND MING K. WANG*

Graduate Institute of Agricultural Chemistry, National Taiwan University, Taipei 106, Taiwan

Abstract—Birnessite can be used as a precursor in the preparation of manganese oxides. Synthesis of pure birnessite is difficult because of a side reaction, which yields hausmannite. This study aimed to develop a modified oxidation-deprotonation reaction (ODPR) method to eliminate the formation of hausmannite, and to investigate the influence of alkalinity on the synthetic products. In contrast to the conventional synthesis of birnessite through oxygen or permanganate oxidation, the ODPR method can produce birnessite without any impurities, within 5 h, and in a reproducible fashion. The distinctive feature of the ODPR method is the bubbling of N₂ gas into NaOH and Mn²⁺ solutions before mixing the NaOH with Mn²⁺, in order to keep oxygen away from each solution. As soon as white pyrochroite was formed, oxygen gas was forced in as an oxidant to initiate the oxidation reaction. A black suspension with a blue tint appeared after 5 h of reaction. These precipitates were collected and examined by X-ray diffraction (XRD), scanning electron microscopy (SEM), infrared (IR) and Raman spectroscopy. The average oxidation state of the Mn oxides was also determined. The results showed that pure birnessite with good crystallinity was formed. Oxidation of 1 M NaOH mixed with Mn²⁺ solution formed random-stacked birnessite. However, the oxidation of 4 M NaOH mixed with Mn²⁺ formed birnessite. Random-stacked birnessite can be transformed into birnessite by ageing suspensions at 313 to 373 K.

Key Words—Birnessite, Pyrochroite, Random Stacked Birnessite, Synthesis.

INTRODUCTION

Birnessites form a group of layered Mn oxides including birnessite, random-stacked birnessite, and hydrated birnessite (1.0 nm) (Giovanoli, 1980). The birnessite minerals are widely distributed in natural environments. For instance, they can be found in mines, soils (Uzochukwu and Dixon, 1986) and Mn nodules on the seafloor (Mandernack and Tebo, 1993).

Among the procedures for synthesis of birnessite reported previously, there are two main approaches. One is to oxidize pyrochroite with oxygen in NaOH solution. This method, proposed by Giovanoli *et al.* (1970a,b), is also known as the OPO method. Another preparation procedure, suggested by McKenzie (1971), is to reduce permanganate using reducing agents in acidic conditions.

In the 1980s, many researchers: Chen *et al.* (1986), Golden *et al.* (1986, 1987), Paterson *et al.* (1986a,b), Cornell and Giovanoli (1988), Kung and McBride (1988), and Post and Veblen (1990), adopted the OPO method to prepare birnessite. However, a side reaction of this method yields hausmannite. Although the conventional OPO method has been employed occasionally to prepare birnessite in the past decade (Manceau *et al.*, 1992; Wong and Cheng, 1992; Drits *et al.*, 1997; Silvester *et al.*, 1997), new methods have been developed as alternatives (Ching *et al.* 1995, 1997; Luo and Suib, 1997; Luo *et al.*, 1998; Ma *et al.*, 1999; Ressler *et al.*, 1999). One common alternative is to oxidize

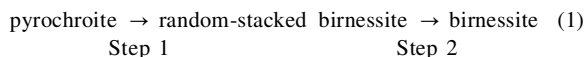
pyrochroite using permanganate (designated as the OPP method) instead of oxygen. However, the OPP method has the disadvantage of being time consuming.

In this study, we developed the oxidation-deprotonation reaction (ODPR) method by modifying the conditions of the conventional OPO method. A merit of this method is that it can prevent the formation of hausmannite. The ODPR method prepares pyrochroite in the absence of Mn³⁺; both NaOH and Mn²⁺ were purged with N₂ gas before they were mixed in order to exclude oxygen from each solution. The precipitates were collected and freeze dried for chemical and spectroscopic analyses.

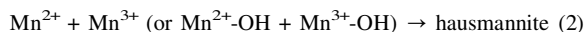
THEORY OF THE OXIDATION-DEPROTONATION REACTION (ODPR) METHOD

The ODPR method was developed by Yang (1996), and is shown in the following equations:

Target reactions:



Side reactions:



Step 1: Mn²⁺ ions are oxidized quickly to Mn⁴⁺, and then hydrolysis occurs converting Mn²⁺-OH to Mn⁴⁺-OH.

Step 2: Random-stacked birnessite or hydrated birnessite suspension ages at high temperature and transforms into birnessite. The temperature ranges between 313 and 373 K.

* E-mail address of corresponding author: mkwang@ccms.ntu.edu.tw

According to the ODP method, whether random-stacked birnessite or hausmannite forms depends on the onset of pyrochroite oxidation. The conversion reaction of pyrochroite into random-stacked birnessite is more favored under fast-oxidation conditions. Thus, the pyrochroite oxidation reaction was carried out under an O_2 flow rate of 5 L min^{-1} for the first 30 min. Thereafter, the flow rate was cut to 1 L min^{-1} and continued for ~5 h.

The formation of hausmannite as a side reaction is influenced by two factors: one is the presence of Mn^{3+} ions before NaOH mixing; the other is temperature. We found that the formation of hausmannite is favored at higher temperature (*i.e.* $>283 \text{ K}$). Hence, maintaining the temperature at $<283 \text{ K}$ can inhibit formation of Mn^{3+} during the mixing of Mn^{2+} and NaOH, thereby improving the quality of birnessite synthesis.

MATERIALS AND METHODS

Chemicals

Reagent-grade chemicals were obtained commercially (Merck, Nacalai) and used without further purification. The distilled deionized water (DDW) used in this study was obtained from a Barnsted Easy Pure water purifying system and used throughout the study.

Syntheses

All manganese oxides (MOs) were prepared by the ODP method. The first step in this procedure is to dissolve 11 g of Mn chips with 100 mL 6 M HCl. The Mn^{2+} solution was then mixed with various quantities of 20.5 M (820 g L^{-1}) NaOH solution to form suspensions of pyrochroite. Pyrochroite suspensions were adjusted to 500 mL with DDW and their NaOH concentrations were set at 1 M, 1.5 M, 2.0 M, and 4 M. The manganese oxides thus formed were designated as 1 M MO, 1.5 M MO, 2.0 M MO and 4 M MO, respectively. In order to remove oxygen from NaOH and Mn^{2+} solutions before they are mixed, both solutions were purged separately, with N_2 gas of high ($>99.9\%$) purity, at a rate of $>0.5 \text{ L min}^{-1}$ for at least 5 min. These two oxygen-free solutions were then blended to form pyrochroite in the absence of Mn^{3+} . The N_2 gas was constantly forced into the pyrochroite suspensions at a rate of $>0.5 \text{ L min}^{-1}$.

The white suspension of pyrochroite was kept at 298 K in a water bath for 30 min. Thereafter, N_2 was immediately replaced by O_2 gas. Oxidation of pyrochroite was achieved by purging with O_2 gas at 298 K. The flow rate of O_2 was set at 5 L min^{-1} for 30 min, and at 1 L min^{-1} for the following 5 h. During the oxidation process, pyrochroite suspensions were stirred vigorously. The speed of mixing was increased to 300 rpm as soon as oxygen bubbling started. Upon completion of all processes, a black suspension with a blue tint was observed. The suspensions aged at 313 to 373 K for at least 5 h. The aged products were centrifuged, and re-

suspended with DDW after discarding the supernatant. These processes were repeated five times to remove all salts and excess NaOH. The precipitates were collected, freeze dried and stored for further analysis.

Characterization

Average oxidation states (AOS) of Mn. Potentiometric titration measurements were used to analyze the AOS of Mn in synthetic products. First, 60 mL of 0.052 M oxalic acid were used to dissolve accurately weighed amounts of birnessites or 5 mL suspension of MOs (in the cases with high concentration of NaOH) and then diluted to 100 mL. The amounts of Mn and excess oxalic acid were determined using an atomic absorption spectrophotometer (AAS) and by titration with a previously standardized 0.03 M $KMnO_4$ solution, respectively. The AOS of Mn in the birnessites were calculated on the basis of these two results.

X-ray diffraction. Two types of XRD were conducted in this work. To check quickly whether birnessites were formed or not, oriented thin-film samples on pieces of filter membrane (a diameter of 25 mm with pore size of $0.45 \mu\text{m}$) were scanned continuously with a scanning rate of 2° min^{-1} with a Rigaku Miniflex X-ray diffractometer. $CuK\alpha$ radiation generated at a tube voltage of 30 kV and a current of 10 mA were used in these oriented-sample runs. To identify various species in all MOs, a Philips PW 1729 X-ray diffractometer was used for powder XRD studies. The $CuK\alpha$ radiation was generated at 40 kV tube voltage and 30 mA tube current. Samples were scanned from $5-60^\circ 2\theta$ steps of $0.02^\circ 2\theta$ at a rate of 5 s per step.

Scanning electron microscopy (SEM). The SEM was performed on gold-coated samples using an Hitachi S-800 field emission scanning electron microscope operated at 20 kV.

Infrared spectroscopy. Transmission IR spectra were obtained using a Bomem model DA8.3. Two ranges, from 4000 to 500 cm^{-1} (middle IR) and 625 to 300 cm^{-1} (far IR), of IR spectra were recorded. The resolution was set at 4 cm^{-1} . In the middle IR range, 200 mg of sample-KBr mixtures (sample:KBr = 1:800) were pressed to form a pellet of 13 mm in diameter. The middle IR spectra were recorded using a mercury cadmium telluride (MCT) detector at a resolution of 4 cm^{-1} . The number of scans was 400. Nitrogen gas was forced into the sample chamber during the scanning period. For far IR measurements, 13 mm diameter pellets were prepared from 40 mg of sample-polyethylene (PE) powder mixtures (sample:PE = 1:200). During the far IR measurements, the sample chamber was evacuated. The resolution and number of scans were the same as those for middle IR experiments, but the spectra were recorded using a deuterated triglycine sulfate (DTGS) detector instead of an MCT detector.

Raman spectroscopy. The Raman spectra were obtained using a Renishaw 2000 micro-Raman system. The excitation source was a 514.5 nm line from a Coherent Innova 90 argon-ion laser. The power of the laser was tuned to 0.2 W but 70% of which was filtered before the laser beam reached the samples. All Raman measurements were carried out in reflection geometry. The samples were pressed gently into pellet form without further treatment.

RESULTS AND DISCUSSION

Behavior of pyrochroite oxidized in NaOH solutions

The MOs prepared from NaOH solutions of 1 M NaOH, 1.5 M NaOH and 4 M NaOH, respectively, are essentially black with AOS in the range 3.77–3.87. The AOS of MO was found to increase with increasing NaOH concentrations. This simple trend is interrupted when $[\text{OH}^-] > 9 \text{ M}$, where the AOS of MO is no longer increased but actually reduced (data not shown). This phenomenon can be explained by oxidation being inhibited in concentrated NaOH solution. The exact mechanism is still unknown. Perhaps the solubility of oxygen is reduced in concentrated NaOH solutions.

Species identification of 1 M MO and 4 M MO

The water content of 1 M–4 M MO ranges from 8.82 to 10.43% (w/w). Conventionally, the excess charges due to Mn^{4+} being replaced by Mn^{3+} are balanced with Na cations. Therefore, from the chemical analysis of AOS and TG measurements, the chemical formula of birnessites prepared in this work is $\text{Na}_x\text{MnO}_2 \cdot y\text{H}_2\text{O}$ ($0.13 < x < 0.23$, $0.49 < y < 0.59$). According to the XRD results (Figure 1), these black MOs were either birnessite or random-stacked birnessite. The MOs prepared in these NaOH concentrations ranging from 4 M to 1 M show two major XRD peaks, 0.71 and 0.36 nm, of birnessite (Figure 1A), and three major XRD peaks, 1.0, 0.51 and 0.34 nm, of hydrated birnessite, respectively (Figure 1B),

in oriented thin films. These XRD peaks are characteristic of birnessite (JCPDS 23-1046) and random-stacked birnessite (Giovanoli *et al.*, 1970a,b). Characteristic XRD peaks arising from hausmannite (Mn_3O_4 , intense XRD peaks at 0.492 nm (101) and 0.249 nm (211)) and feitknechtite ($\beta\text{-MnOOH}$) are strongest at 0.462 nm, which corresponds to (002), due to its platy structure. This assumption is also confirmed by SEM studies. As seen in SEM photographs (Figure 2), in the case of 1 M MO (Figure 2a), the MO materials are stacked as random flower petals. In contrast, only well-stacked pellets a few μm in size can be observed for 4 M MO (Figure 2b). The results of the 1.5 M and 2.0 M MO are not shown in Figures 1 and 2, but their characteristics are closer to those of 1 M MO.

The powder XRD pattern (Figure 3) further suggests that MOs synthesized by pyrochroite oxidized in 1 M and 4 M NaOH solutions are random-stacked birnessite and birnessite, respectively. As can be seen, hydrated birnessite was dehydrated and its 1 nm *d*-spacing was reduced to 0.7 nm (Luo *et al.*, 1998) while being freeze dried. Figure 3a displays the 4 M MO XRD pattern in the range of 5 to $70^\circ 2\theta$. The powder XRD pattern of synthetic birnessite showed very intense XRD peaks at *d*-spacings 0.71, 0.36, 0.25, 0.24, 0.22, 0.21, 0.19, 0.18, 0.16, 0.15 and 0.14 nm (JCPDS 23-1046). These 11 XRD peaks are characteristic of pure birnessite (Giovanoli *et al.*, 1970a,b) and there is no evidence of the formation of hausmannite (JCPDS 24-734) or feitknechtite (JCPDS 18-804). The XRD pattern in Figure 3a in the range 30 – $70^\circ 2\theta$ is magnified and shown in Figure 3b. It coincides essentially with the Na-birnessite XRD pattern observed by Post and Veblen (1990).

Hence, all results shown indicate that the products obtained in the range 1 M NaOH (1 M MO) to 4 M NaOH (4 M MO) solutions consist essentially of birnessites (random-stacked birnessite and birnessite) with no XRD-detectable impurities.

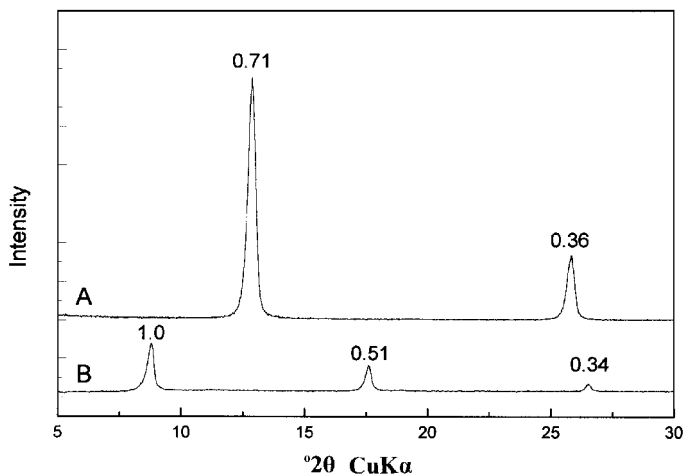


Figure 1. Comparison of XRD patterns of (A) 4 M MO (birnessite) and (B) 1 M MO (random-stacked birnessite).

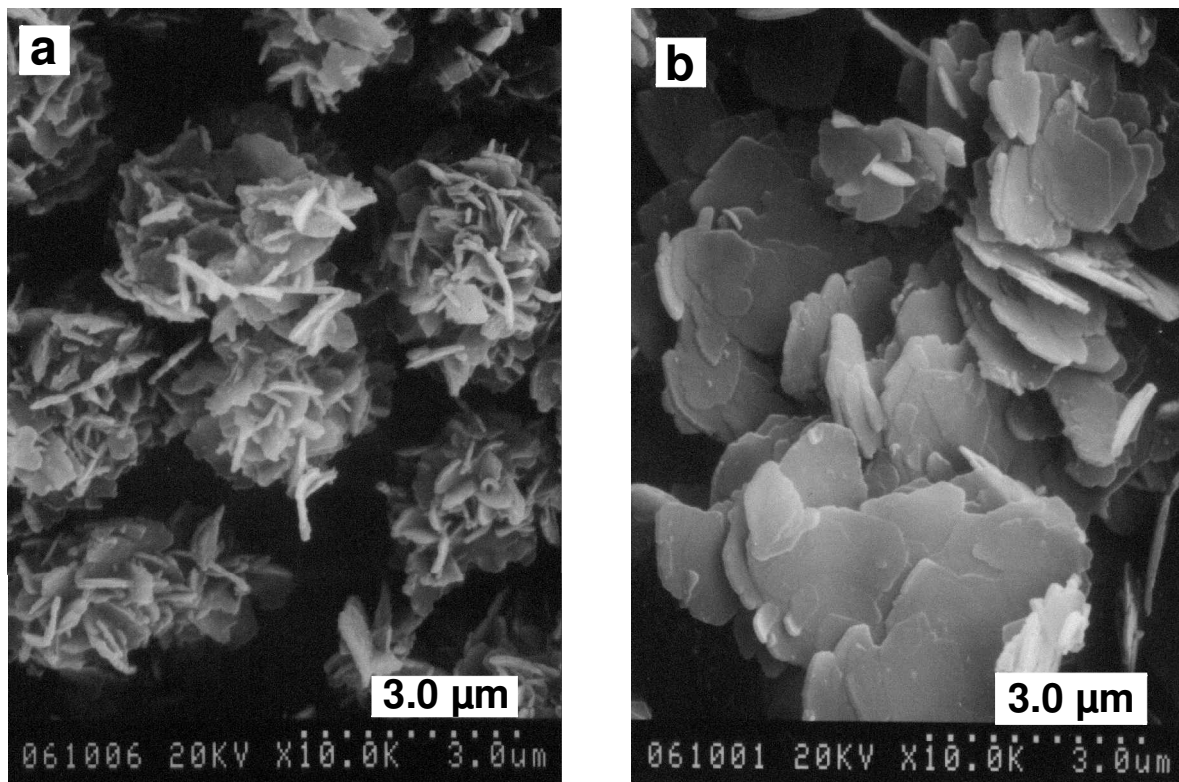


Figure 2. Scanning electron micrographs of (a) 1 M MO (random-stacked birnessite) and (b) 4 M MO (birnessite).

Short-range structural relationships between birnessite and random-stacked birnessite

Burns *et al.* (1983) and Giovanoli (1985) raised the issue of the definition of terms and structural relationships between birnessite, random-stacked birnessite and todorokite. In this work, random-stacked birnessite is used as defined by Giovanoli (1980). As discussed above, the relationships between 1 M MO

and 4 M MO are in line with the long-range structural relationships between vernadite and birnessite (refer to results shown in Figures 1, 2 and 3). However, short-range structural relationships between these two minerals have never been examined carefully. Thus, IR and Raman spectroscopic studies of 1 M MO and 4 M MO (random-stacked birnessite and birnessite) were performed to study their short-range structural relationships.

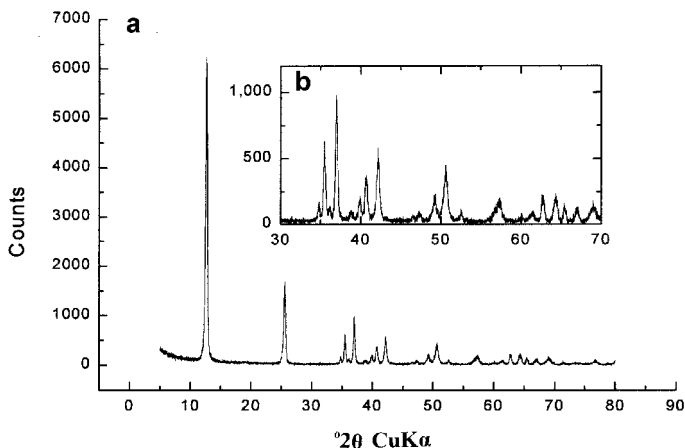


Figure 3. Powder XRD patterns of 4 M MO (birnessite). (a) 5–70°2θ; (b) 30–70°2θ.

To compare the short-range structures between random-stacked birnessite and birnessite, interlayer water and Mn octahedral sheets were studied. Potter and Rossman (1979) reported the IR data and discussed the interlayer water in birnessite. They suggested that a band occurring at $\sim 3400\text{ cm}^{-1}$ was due to hydroxide ions in specific crystallographic sites, and less-ordered water produces the remaining features in the range 3600 to 2800 cm^{-1} . Other studies used chemical analysis, XRD, selected-area electron diffraction (SAED), difference-Fourier maps and extended X-ray absorption fine structure (EXAFS) to examine birnessite and had similar conclusions with regard to interlayer water (Post and Veblen, 1990; Drits *et al.*, 1997; Silvester *et al.*, 1997). Thus, water has been recognized as the predominant interlayer molecule in birnessites.

The IR spectra of random-stacked birnessite and birnessite in the range 4000 to 1500 cm^{-1} are generally in agreement with those of previous works (Potter and Rossman, 1979). Asymmetric broad bands in the range 3600 to 2800 cm^{-1} and a weaker broad band at 1633 cm^{-1} support the argument that interlayer water exists in birnessites. The IR bands of random-stacked birnessite and birnessite (data not shown) are analogous to each other.

The IR and Raman spectra of Mn octahedral sheets of random-stacked birnessite and birnessite are shown in

Figures 4 and 5, respectively. As seen in these two figures, all but the Raman line at 637 cm^{-1} in Figure 5A and 652 cm^{-1} in Figure 5B correspond to Mn–O stretching vibrations. Owing to the similarity of IR and Raman spectra between vernadite and birnessite, the short-range arrangements of Mn octahedral sheets of random-stacked birnessite and birnessite also show great similarity. The line shift observed in the Raman spectra may be caused by differences in crystallinity.

Both the interlayer water and Mn octahedral sheets in random-stacked birnessite and birnessite have quite similar configurations. Consequently, whether viewed from a long-range or short-range scale, the structure of random-stacked birnessite is similar to that of birnessite except for the layer arrangement. Thus, vernadite is a random-stacked birnessite (Giovanoli, 1980).

Mechanism of birnessite formed by the ODPR method

Figures 1, 2 and 3 show that the MOs synthesized in this work essentially consisted of birnessite or vernadite, depending on NaOH concentrations (in the range of 1 M to 4 M) while pyrochroite was oxidized. Such pure birnessites (including random-stacked birnessite and hydrated birnessite) could be obtained within 5 h. Comparing the ODPR and OPP methods, revealed two coincidences. Luo *et al.* (1998) reported that the product prepared at low basicity ($[\text{OH}^-] = 1.6\text{ mol L}^{-1}$, our work

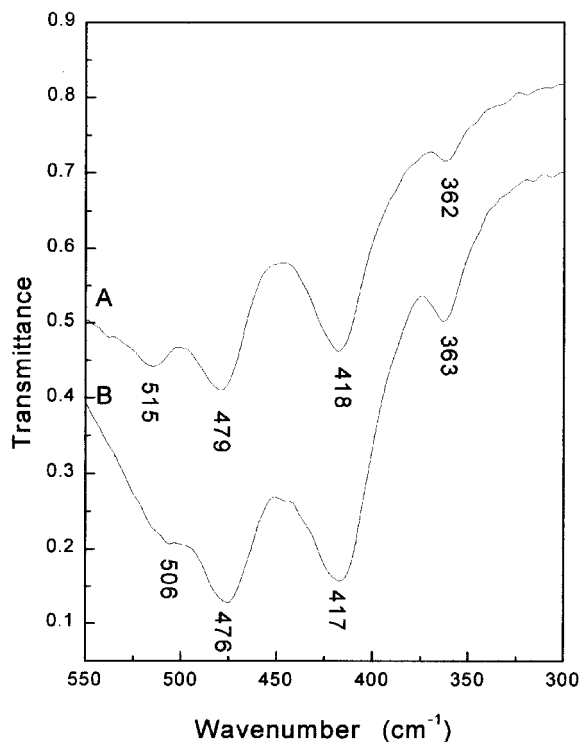


Figure 4. Comparison of IR spectra of (A) 1 M MO (random-stacked birnessite) and (B) 4 M MO (birnessite) in the range 550 – 300 cm^{-1} .

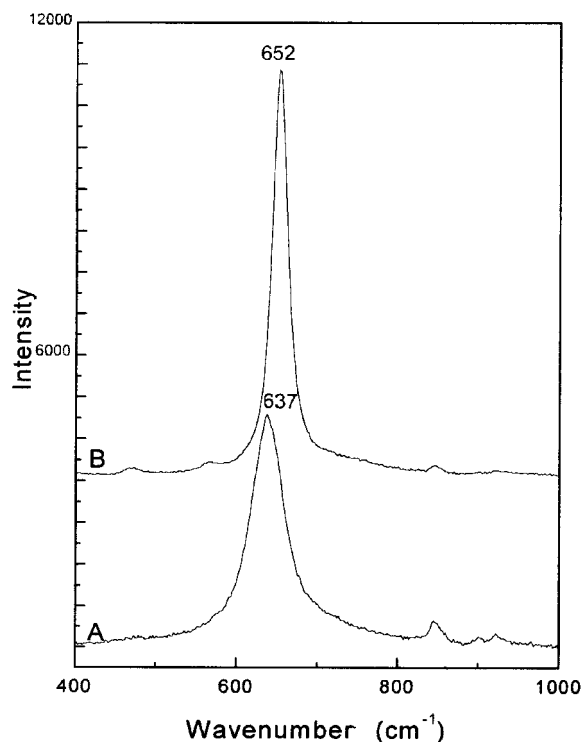


Figure 5. Comparison of Raman spectra of (A) 1 M MO (random-stacked birnessite) and (B) 4 M MO (birnessite) in the range 1000 – 400 cm^{-1} .

$[\text{OH}^-] = 1 \text{ mol L}^{-1}$) has a flower-like platy morphology, while that prepared at high basicity ($[\text{OH}^-] = 3.6 \text{ mol L}^{-1}$, this work $[\text{OH}^-] = 4 \text{ mol L}^{-1}$) is made up of hexagonal platy crystallites. This description (Luo and Suib, 1997) can also be applied to our results, as shown in Figure 2. These coincidences imply that the ODPR and the OPP methods have similar reaction mechanisms. Luo *et al.* (1998) proposed a possible route for the synthesis of birnessite as follows:

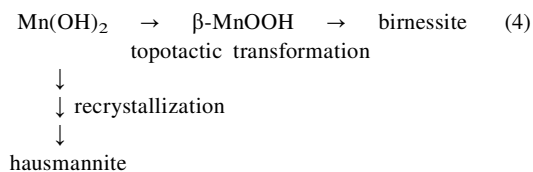


The MnO_x , proposed as a hausmannite-related material, was formed during an induction period (Luo and Suib, 1997). It may be stable for a long period of time before transformation occurs and such an induction period can be shortened by increasing either the temperature or basicity (Luo and Suib, 1997; Luo *et al.*, 1998). Equation 3 is not unique to the ODPR method. Cornell and Giovanoli (1988) made similar observations. However, equation 3 can fit both conventional OPO and OPP methods. Cornell and Giovanoli (1988) reported that MnO_x prepared by the conventional OPO method could be transformed into birnessite in 1 M KOH at 343 K. Such a transformation may take weeks or months to complete. Thus, the OPP method is also time-consuming, like the conventional OPO method.

Giovanoli *et al.* (1970a,b), McKenzie (1971), Post and Veblen (1990), Drits *et al.* (1997) and Silvester *et al.* (1997) reported that birnessite can be obtained in 5 h using the conventional OPO method. The difference in the time required by the various methods is notable. Thus, with the conventional OPO method, the formation of birnessite may involve a topotactic transformation (Cornell and Giovanoli, 1988) from pyrochroite.

Conditions favoring formation of birnessite

As reported in previous studies, a side reaction occurs, forming hausmannite, when birnessite is prepared by oxidizing pyrochroite with oxygen under alkaline conditions (equation 4).



To obtain pure birnessite, it is necessary to eliminate the side reaction of hausmannite formation. Using the conventional OPO method, keeping the temperature close to 283 K favors the formation of birnessites. On the other hand, the ODPR method prepares random-stacked birnessite or hydrated birnessite by adjusting the concentration of NaOH solutions. The random-stacked birnessite or hydrated birnessite can transform into birnessite without any impurities after aging the suspensions at 313 to 373 K. Besides these two

conditions above, our current work shows that anions may also affect the crystallinity of birnessite.

CONCLUSIONS

The average oxidation states of pyrochroite suspensions are close to 2. Addition of 1 M [NaOH] to Mn^{2+} solution yields random-stacked birnessite. On the other hand, using 4 M [NaOH], hydrated birnessite is formed after 5 h of oxidation treatment. According to IR and Raman measurements, random-stacked birnessite and birnessite are not only similar in the long-range order of atomic arrangements, but also on a short-range scale.

With the ODPR method, 'XRD-pure' birnessites can be obtained within a short time. The ODPR method requires less time to synthesize birnessite than the conventional OPP and OPO methods, and yields reproducible products. With the ODPR method, birnessite can be synthesized at 313 to 373 K.

ACKNOWLEDGMENTS

We acknowledge financial support from the National Science Council of the ROC, under project #NSC89-2621-B002-006.

REFERENCES

- Burns, R.G., Burns, V.M. and Stockman, H.W. (1983) A review of the todorokite–buserite problem: Implications to the mineralogy of marine manganese nodules. *American Mineralogist*, **68**, 972–980.
- Chen, C.C., Golden, D.C. and Dixon, J.B. (1986) Transformation of synthetic birnessite to cryptomelane: An electron microscopy study. *Clays and Clay Minerals*, **34**, 565–571.
- Ching, S., Landrigan, J.A. and Jørgensen, M.L. (1995) Sol-gel synthesis of birnessite from KMnO_4 and simple sugar. *Chemistry of Materials*, **7**, 1064–1066.
- Ching, S., Petrovay, D.J., Jørgensen, M.L. and Suib, S.L. (1997) Sol-gel synthesis of layered birnessite-type manganese oxides. *Inorganic Chemistry*, **36**, 883–890.
- Cornell, R.M. and Giovanoli, R. (1988) Transformation of hausmannite into birnessite in alkaline media. *Clays and Clay Minerals*, **36**, 249–257.
- Drits, V.A., Silvester, E., Gorshkov, A.I. and Manceau, A. (1997) Structure of synthetic monoclinic Na-rich birnessite and hexagonal birnessite: I. Results from X-ray diffraction and selected-area electron diffraction. *American Mineralogist*, **82**, 946–961.
- Giovanoli, R. (1980) Vernadite is random-stacked birnessite. *Mineralium Deposita*, **14**, 249–261.
- Giovanoli, R. (1985) Layer structures and tunnel structures in manganates. *Chemie der Erde*, **44**, 227–244.
- Giovanoli, R., Stahli, E. and Feitknecht, W. (1970a) Ueber oxidhydroxide des vierwertigen mangans mit schichtengitter. 1. Mitteilung: Natriummangan (II, III) manganat(IV). *Helvetica Chimica Acta*, **53**, 209–220.
- Giovanoli, R., Stahli, E. and Feitknecht, W. (1970b) Ueber oxidhydroxide des vierwertigen mangans mit schichtengitter. 1. Mitteilung: Natriummangan (II, III) manganat(IV). *Helvetica Chimica Acta*, **53**, 453–464.
- Golden, D.C., Dixon, J.B. and Chen, C.C. (1986) Ion exchange, thermal transformations, and oxidizing properties

- of birnessite. *Clays and Clay Minerals*, **34**, 511–520.
- Golden, D.C., Chen, C.C. and Dixon, J.B. (1987) Transformation of birnessite to buserite, todorokite, and manganite under mild hydrothermal treatment. *Clays and Clay Minerals*, **35**, 271–280.
- Kung, K.-H. and McBride, M.B. (1988) Electron transfer process between hydroquinone and hausmannite. *Clays and Clay Minerals*, **36**, 297–302.
- Luo, J. and Suib, S.L. (1997) Preparative parameters, magnesium effects, and anion effects in the crystallization of birnessites. *Journal of Physical Chemistry B*, **101**, 10403–10413.
- Luo, J., Huang, A., Park, S.H., Suib, S.L. and O'Young, C.-L. (1998) Crystallization of sodium-birnessite and accompanied phase transformation. *Chemistry of Materials*, **10**, 1561–1568.
- Ma, Y., Luo, J. and Suib, S.L. (1999) Syntheses of birnessites using alcohols as reducing reagents: Effects of synthesis parameters on the formation of birnessites. *Chemistry of Materials*, **11**, 1972–1979.
- Manceau, A., Gorshkov, A.I. and Drits, V.A. (1992) Structural chemistry of Mn, Fe, Co, and Ni in manganese hydrous oxides: Part I. Information from XANES spectroscopy. *American Mineralogist*, **77**, 1133–1143.
- Mandernack, K.W. and Tebo, B.M. (1993) Manganese scavenging and oxidation at hydrothermal vents and in vent plumes. *Geochimica et Cosmochimica Acta*, **57**, 3907–3923.
- McKenzie, R.M. (1971) The synthesis of birnessite, cryptomelane, and some other oxides and hydroxides of manganese. *Mineralogical Magazine*, **38**, 493–502.
- Paterson, E., Bunch, J.L. and Clark, D.R. (1986a) Cation exchange in synthetic manganates. I. Alkylammonium exchange in a synthetic phyllosmanganate. *Clay Minerals*, **21**, 949–955.
- Paterson, E., Clark, D.R., Russell, J.D. and Swaffield, R. (1986b) Cation exchange in synthetic manganates. II. The structure of an alkylammonium-saturated phyllosmanganate. *Clay Minerals*, **21**, 957–964.
- Post, J.E. and Veblen, D.R. (1990) Crystal structure determinations of synthetic sodium, magnesium, and potassium birnessite using TEM and the Rietveld method. *American Mineralogist*, **75**, 477–489.
- Potter, R.M. and Rossman, G.R. (1979) The tetravalent manganese oxides: Identification, hydration, and structural relationships by infrared spectroscopy. *American Mineralogist*, **64**, 1199–1218.
- Ressler, T., Brock, S.L., Wong, J. and Suib, S.L. (1999) Multiple-scattering EXAFS analysis of tetraalkylammonium manganese oxide colloids. *Journal of Physical Chemistry B*, **103**, 6407–6420.
- Silvester, E., Manceau, A. and Drits, V.A. (1997) Structure of synthetic monoclinic Na-rich birnessite and hexagonal birnessite: II. Results from chemical studies and EXAFS spectroscopy. *American Mineralogist*, **82**, 962–978.
- Uzochukwu, G.A. and Dixon, J.B. (1986) Manganese oxide minerals in nodules of two soils of Texas and Alabama. *Soil Science Society of American Journal*, **50**, 1079–1084.
- Wong, S.-T. and Cheng, S. (1992) Synthesis and characterization of pillared buserite. *Inorganic Chemistry*, **31**, 1165–1172.
- Yang, D.S. (1996) Structural properties phyllosmanganates and its application to their identification in soils. Ph.D. thesis. National Taiwan University, p. 216.

(Received 16 October 2000; revised 12 June 2001; Ms. 493)